

# Closed-Tube Genotyping with Unlabeled Oligonucleotide Probes and a Saturating DNA Dye

LUMING ZHOU, ALEXANDER N. MYERS, JOSHUA G. VANDERSTEEN, LESI WANG, and  
CARL T. WITTWER\*

**Background:** Homogeneous PCR methods for genotyping usually require fluorescently labeled oligonucleotide probes. Amplicon melting with the DNA dye LCGreen<sup>TM</sup> I was recently introduced as a closed-tube method of genotyping that does not require probes or real-time PCR. However, some single-nucleotide polymorphisms (SNPs) could not be completely genotyped without addition of a known genotype, and high-resolution melting techniques were necessary.

**Methods:** A 3'-blocked, unlabeled oligonucleotide probe and the saturating dye, LCGreen I, were added to standard PCR reagents before amplification. After PCR, the samples were melted at 0.1–0.3 °C/s in high-resolution (HR-1<sup>TM</sup>), high-throughput (LightTyper<sup>TM</sup>), and rapid-cycle, real-time (LightCycler<sup>®</sup>) instruments, and fluorescence melting curves were recorded.

**Results:** Derivative melting curves of the probe–target duplexes were characteristic of the genotype under the probe. With synthetic plasmid templates, all SNP base combinations could be genotyped. For human genomic DNA, the technique was demonstrated with mutations associated with cystic fibrosis, including SNPs (G542X, I506V, and F508C) and 3-bp deletions (F508del and I507del).

**Conclusions:** Genotyping of SNPs and small deletions by melting analysis of an unlabeled probe in the presence of LCGreen I is simple and rapid. Only three unlabeled oligonucleotides (two primers and one probe), a saturating DNA dye, PCR, and a melting instrument are required. The method is closed-tube,

does not require fluorescently labeled probes or real-time PCR, and can be completed in <10 min on any instrument capable of monitoring melting curves by fluorescence.

© 2004 American Association for Clinical Chemistry

There are many methods to genotype small sequence alterations such as single-nucleotide polymorphisms (SNPs). Most methods first amplify the DNA region of interest by PCR. Analysis of the PCR fragments ranges from simple manual methods, such as restriction enzyme digestion with separation on agarose gels, to complex techniques using a mass spectrometer that can, nevertheless, be automated. Homogeneous methods that do not require any processing after addition of target DNA are attractive because no automation is necessary. Such “closed-tube” techniques usually use fluorescently labeled oligonucleotide probes. Examples include methods based on probe melting (1–3) and 5'-exonuclease digestion of probes (4). Genotyping by melting analysis is advantageous because multiple alleles can be analyzed with one probe (5), whereas other methods require one probe for each allele. Homogeneous methods are simple, fast (<30 min, including PCR), and prevent the release of PCR products into the environment (6). However, the required design and expense of fluorescently labeled probes are disadvantages.

Homogeneous melting of PCR products in the presence of the DNA dye LCGreen<sup>TM</sup> I can detect heterozygotes and genotype SNPs (7). Heterozygotes are identified by a change in melting curve shape, and different homozygotes are distinguished by a change in melting temperature ( $T_m$ ). Unlike other commonly used dyes in real-time PCR, LCGreen I can be used at high concentrations that saturate PCR products without inhibiting amplification. Multiple products with different  $T_m$ s are easily detected with LCGreen I, whereas higher  $T_m$  products are

Department of Pathology, University of Utah School of Medicine, Salt Lake City, UT.

\*Address correspondence to this author at: Department of Pathology, University of Utah School of Medicine, Salt Lake City, UT 84132. Fax 801-581-4517; e-mail carl.wittwer@path.utah.edu.

Received March 16, 2004; accepted April 30, 2004.

Previously published online at DOI: 10.1373/clinchem.2004.034322

preferentially detected with SYBR<sup>®</sup> Green I. The bias of SYBR Green I toward higher  $T_m$  products has been attributed to redistribution of dye during melting (8) and bias toward GC-rich sequences (9).

A recent study of SNP genotyping with LCGreen I used small amplicons to increase the  $T_m$  difference between homozygous genotypes (10). Heterozygotes were easy to identify in all cases. In SNPs in which a G::C base pair was interchanged with an A::T base pair (84% of human SNPs), the  $T_m$  difference between homozygous genotypes (~1 °C) could be distinguished on standard melting instruments. However, in the remaining cases, in which only the base pair orientation changed (A::T to T::A or G::C to C::G), high-resolution melting was necessary to differentiate homozygotes. Furthermore, in one fourth of these cases (4% of human SNPs), addition of a known genotype was necessary.

Genotyping by amplicon melting depends on the specificity of the PCR primers. At least in clinical assays, it is commonly believed that the extra specificity of a probe is necessary. To provide probe specificity without the cost of a fluorescently labeled oligonucleotide, we investigated the feasibility of genotyping with unlabeled oligonucleotide probes with use of asymmetric PCR and LCGreen I. The result is a closed-tube, homogeneous method for genotyping without fluorescently labeled probes or allele-specific PCR (11, 12). Either conventional real-time PCR instruments or more economic, dedicated melting instruments can be used. High-resolution analysis is not necessary, and any SNP can be genotyped by use of three unlabeled oligonucleotides in one reaction.

### Materials and Methods

#### DNA SAMPLES

Engineered plasmids with an A, C, G, or T at a defined position amid 40% GC sequences (13) were kindly provided by Cambrex BioScience Rockland, Inc. (Rockland, ME). Human genomic DNA was obtained from a previous study (14) or from the Coriell Institute for Medical Research. Genomic DNA and plasmids were quantified by  $A_{260}$ .

#### $T_m$ CALCULATIONS

Duplex  $T_m$ s were calculated by use of previously described nearest-neighbor thermodynamic models (15–22) and custom software. The best fit for the  $Mg^{2+}$  equivalence (74-fold that of  $Na^+$ ) was obtained by use of a data set of 475 duplexes (23). The amplicon concentration at the end of PCR was set at the limiting primer concentration. The effective concentration of  $Mg^{2+}$  was decreased by the total deoxynucleotide triphosphate concentration, assuming stoichiometric chelation. The effect of  $Tris^+$  was assumed equal to  $Na^+$ , and the  $Tris^+$  concentration (20 mmol/L) was calculated from the buffer concentration and pH. Oligonucleotides were obtained from the University of Utah Core facility.

#### ASYMMETRIC PCR

PCR of the engineered plasmids and the genomic samples was performed in 10- $\mu$ L reaction volumes with 50 mM Tris (pH 8.3), 500  $\mu$ g/mL bovine serum albumin, 3 mM  $MgCl_2$ , 200  $\mu$ M of each deoxynucleotide triphosphate, 0.4 U of Taq Polymerase (Roche Applied Science), 1 $\times$  LCGreen I (Idaho Technology), 0.5  $\mu$ M excess primer, 0.5  $\mu$ M probe, and 0.05  $\mu$ M limiting primer, unless otherwise stated. In some experiments, SYBR<sup>®</sup> Green I at a final concentration of 1 $\times$  (Molecular Probes) replaced LCGreen I. The plasmids were used at 10<sup>6</sup> copies, and PCR was performed in a LightCycler<sup>®</sup> for 45 cycles with denaturation at 95 °C (0 s hold), annealing at 55 °C (0 s hold), and extension at 72 °C (10 s hold). Transition rates between temperatures were programmed at 20 °C/s, and fluorescence was acquired at the end of extension. When a plasmid "heterozygote" was amplified, equal amounts of each template (25 ng) were used. The primers (13) were 5'-GATATTTGAAGTCTTTCCGGG-3' (0.05  $\mu$ M) and 5'-TAAGAGCAACACTATCATAA-3' (0.5  $\mu$ M) and amplified a 300-bp product. The variable site was in the center of the PCR product. The longest probe was 30 bases long (5'-GGGGGATTCAATGAAATATTTATGACGATTC-P-3'), in which the variable site is underlined and "-P" indicates a 3' phosphate. Shorter probes from 28 to 14 bases were also used with 1–8 bases removed from each end, all with 3' phosphates.

For amplification of the cystic fibrosis sequence variants, 50 ng of genomic DNA was initially denatured at 95 °C for 10 s, followed by 45 cycles of 95 °C with a 0 s hold, 52 °C with a 0 s hold, and 72 °C with a 10 s hold. The exon 10 target (201 bp) was amplified with primers 5'-ACTTCTAATGATGATTATGGG-3' (0.05  $\mu$ M) and 5'-ACATAGTTTCTTACCTCTTC-3' (0.5  $\mu$ M) with probe 5'-TAAAGAAAATATCATCTTTGGTGTTTCCTA-P-3'. The exon 11 target (198 bp) was amplified with primers 5'-TGTGCCTTTCAAATTCAGATTG-3' (0.05  $\mu$ M) and 5'-CAGCAAATGCTTGCTAGACC-3' (0.5  $\mu$ M). For exon 11, one of two probes was used, 5'-CAATATAGTTCTTX-GAGAAGGTGGAATC-P-3', with X being either G or T.

#### MELTING CURVE ACQUISITION AND ANALYSIS

Melting analysis was performed on three different instruments. Melting analysis on the LightCycler immediately followed amplification with an additional denaturation at 95 °C with a 0 s hold, cooling at a programmed rate of 20 °C/s to 40 °C with a 0 s hold, and continuous melting curve acquisition during a 0.2 °C/s ramp to 90 °C. A derivative melting curve plot was obtained with use of default settings of the LightCycler software.

For melting analysis on the high-resolution melting instrument (HR-1<sup>TM</sup>; Idaho Technology), the amplified samples were first denatured (95 °C with no hold) and rapidly cooled to 40 °C at 20 °C/s in the LightCycler. The capillary samples were then removed from the LightCycler, placed in the HR-1 instrument, and melted at

0.3 °C/s. The data were then displayed as derivative melting curve plots by the HR-1 analysis software.

Melting analysis on the LightTyper™ (Roche) was performed after modification of the standard instrument to match the optics to the LCGreen I dye. The standard 470 nm excitation light-emitting diodes were replaced with 450 nm light-emitting diodes (Bright-LED Optoelectronics). In addition, the optical filters were changed to a 425–475 excitation filter and a 485 nm long-pass filter (both from Omega Optical). Amplified samples were denatured and cooled in the LightCycler as described above for the HR-1 instrument. The samples were then removed from the LightCycler capillaries by centrifugation, placed in a 384-well microtiter tray, overlaid with 10  $\mu$ L of mineral oil, and melted at 0.1 °C/s. Data were exported into HR-1 analysis software through a custom interface, and derivative melting curve plots were displayed.

### Results

The effect of primer asymmetry on “real-time” PCR (fluorescence monitored each cycle) and on post-PCR melting analysis is shown in Fig. 1. When the primer concentrations were equal, fluorescence appeared earlier and reached higher plateaus than when one of the primer concentrations was limiting (Fig. 1A). Derivative melting plots of PCR products after symmetric amplification showed large peaks characteristic of the double-stranded DNA amplified (24). The peak from double-stranded amplicon decreased when either one of the primer concentrations was limited (Fig. 1B). When the two opposite asymmetric amplification products were mixed together after PCR, a large peak from the double-stranded amplicon reappeared (data not shown). When the strand complementary to an oligonucleotide probe was produced in excess, a probe–target duplex peak appeared that could be used for genotyping under the probe sequence.

The peak height of the probe–target signal depended on the concentrations of (a) the probe, (b) the complementary PCR product strand, and (c) the opposite competing PCR strand. The concentrations of the two PCR product strands depended on the degree of asymmetry and the number of temperature cycles after the PCR plateau. We found that 10-fold primer asymmetry with 10 cycles after the plateau was optimal (data not shown), and these conditions were used in the experiments that follow. The peak heights of the PCR product and probe–target signals also depended on their lengths. Long PCR products tended to obscure the probe–target peak, and asymmetric PCR was absolutely necessary. The relative magnitude of the probe–target transition increased as the amplicon length decreased, and PCR products <100 bp did not always require asymmetric amplification.

The effect of probe length on detecting the probe–target duplex is shown in Fig. 2. Oligonucleotide probes were added before PCR, and melting curves were ob-

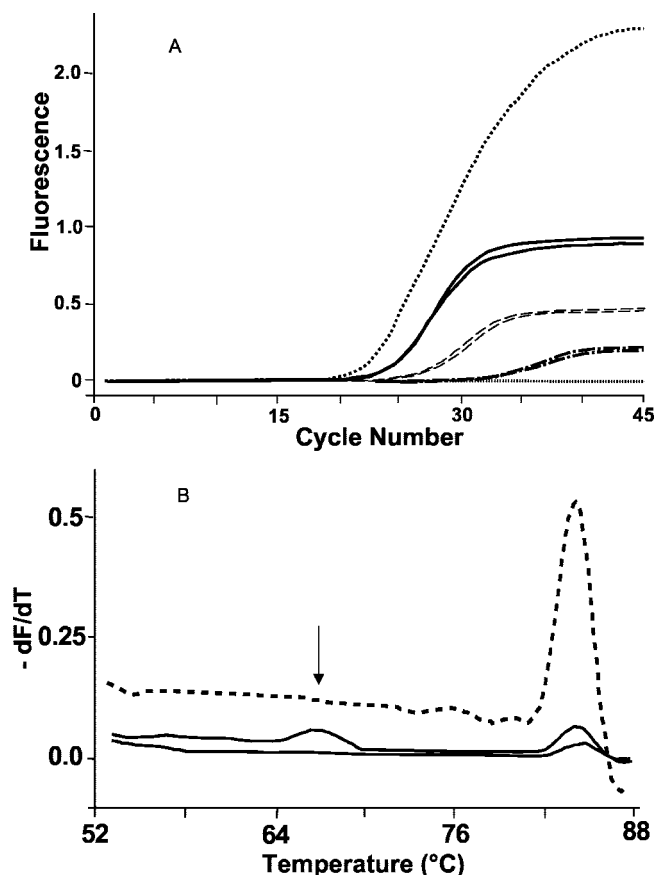


Fig. 1. Real-time (A) and derivative (B) melting curves resulting from symmetric and asymmetric PCR in the presence of an unlabeled oligonucleotide probe and LCGreen I.

The probe was 28 bases long and perfectly matched the 300-bp template. In panel A, the fluorescence of reactions at different degrees of primer asymmetry was monitored each cycle in the F1 channel of the LightCycler. The strongest fluorescence was observed with symmetric PCR (0.5  $\mu$ M each primer; *darker dotted line*). Primer asymmetry ratios tested were 1:10 (both directions; *solid lines*), 1:20 (both directions; *dashed lines*), and 1:50 (both directions; *dot-dashed line*), keeping the excess primer at 0.5  $\mu$ M. A reaction without template (symmetric primers at 0.5  $\mu$ Mol/L each) is also shown (*light dotted line*). As the primer asymmetry increases, the amplification efficiency and the plateau fluorescence decrease, whereas the second derivative maximum (6) increases. Shown in panel B are the derivative melting curves of the symmetric and the two 1:10 asymmetric reactions, as obtained on the LightCycler. The *prominent peak* resulting from the symmetric amplification is the 300-bp PCR product. The asymmetric amplifications produce much less double-stranded PCR product. The small peak at 67 °C present in one of the asymmetric amplifications is the probe melting from single-stranded target (*arrow*). Probe melting peaks are not present in the symmetric or opposite asymmetric amplifications.

tained after amplification. Probes 22–30 bases long (GC content, 27–37%) with no mismatch to the template melted between 60 and 70 °C with distinct peaks on derivative plots. Nearest-neighbor  $T_m$  predictions (22) underestimated these  $T_m$ s by  $\sim$ 4 °C (range, 56.2–66.6 °C). Although matched probes of 14–20 bases were detectable, the peak heights decreased with probe length. When the probe was mismatched to the template at 1 base near the center, the lowest detectable length was 22 bp (data not shown).

In additional experiments, we assessed the usefulness of probes with extreme GC content (0% and 100%) by use

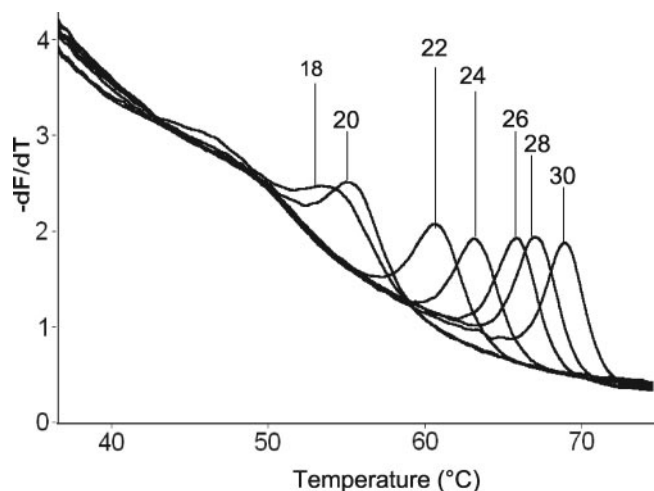


Fig. 2. Derivative melting curves obtained with perfectly matched unlabeled probes of different lengths.

A 1:10 asymmetric PCR was performed as described in the legend for Fig. 1 with probes between 18 and 30 bases long. Melting analysis was performed on the high-resolution instrument, HR-1, and a derivative plot was obtained. The HR-1 signal is ~20 times stronger than the signal obtained on the LightCycler because the HR-1 optics are better matched to the dye LCGreen I. The numbers indicate the probe lengths.

of synthetic oligonucleotide targets. With probes 40 bases long, both 100% AT and 100% GC sequences were detected with  $T_m$ s of 55 and 91 °C, respectively (derivative plots not shown). The peak height of the 100% GC probe was lower than that of the 100% AT probe, which is at least partly explained by the expected decrease in fluorescence with increasing temperature. When the GC content was 100%, probes as small as 10 bases were easily detected ( $T_m$ , 48 °C; derivative plots not shown). Probes 27–30 bases long with 40–60% GC content were routinely used in the remaining experiments, giving  $T_m$ s between 55 and 70 °C.

Engineered plasmids (14) were used to study all possible SNP base combinations. Four plasmids (identical except for an A, a C, a G, or a T at one position) were either used alone to simulate homozygous genotypes or in binary combinations to construct simulated heterozygotes. When we used an A in a 28mer probe at the variable position, we obtained the derivative melting curves shown in Fig. 3 for all homozygotes and heterozygotes after PCR amplification. All homozygotes melted in a single transition (Fig. 3, top curve set). The A::T match was most stable, with a  $T_m$  of 66.1 °C (predicted, 64.0 °C), with the mismatches A::G ( $T_m$  of 63.0 °C; predicted, 62.4 °C), A::A ( $T_m$  of 61.9 °C; predicted, 60.7 °C), and A::C ( $T_m$  of 61.4 °C; predicted, 60.8 °C) decreasing in order of stability. Heterozygous templates with one allele matched to the probe clearly displayed two peaks (Fig. 3, middle curve set). The higher temperature peak corresponded to the perfectly matched duplex and the lower temperature peak to a duplex with a 1-base mismatch. Heterozygous templates with neither of the alleles matched to the probe usually produced an apparent broad single transition

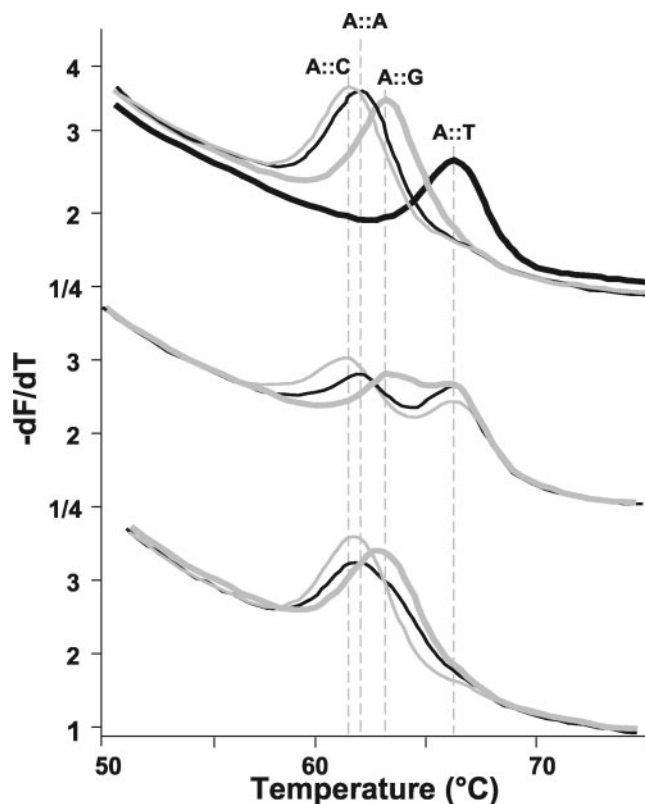


Fig. 3. Derivative melting curve plots of all possible SNP genotypes at one position, obtained with engineered plasmids and a 28-base, unlabeled oligonucleotide probe.

The probe has an A at the variable site and hybridizes to plasmids with an opposing A, C, G, or T. In the top curve set, each of the four plasmids was amplified separately in the presence of the probe, simulating homozygous genotypes. The most stable duplex results from an A::T match with the product (thick black line), followed by A::G (thick gray line), A::A (thin black line), and A::C (thin gray line) mismatches. To simulate heterozygotes, two plasmids were mixed in equal proportions (middle curve set). One of the plasmids is completely complementary to the probe, whereas the other produces A::G (thick gray line), A::A (thin black line), or A::C (thin gray line) mismatches. In the bottom curve set, both plasmids are mismatched to the probe, producing A::G and A::A (thick gray line), A::G and A::C (thin black line), or A::C and A::A (thin gray line) mismatches. The HR-1 instrument was used to obtain the melting curves.

(Fig. 3, bottom curve set) with the peaks generally positioned between the relevant two mismatch peaks shown in the middle curve set of Fig. 3. Probes with a C, G, or T in the probe at the variable position gave similar results (data not shown). When SYBR Green I was used instead of LCGreen I, heterozygotes could not be distinguished from homozygotes (data not shown).

SNP genotyping with unlabeled probes and LCGreen I from genomic DNA is shown in Fig. 4. After PCR amplification, three different instruments were used to genotype the cystic fibrosis mutation G542X (a G-to-T transversion) with two different probes. The top row in Fig. 4 displays derivative melting curves using a probe matched to the wild type, whereas the bottom row shows the curves obtained with a probe matched to the mutation. In all cases, genotyping was clear, although the resolution decreased in the following order: HR-1 > LightTyper > LightCycler. The predicted  $T_m$ s (G::C = 65.9 °C, G::A =

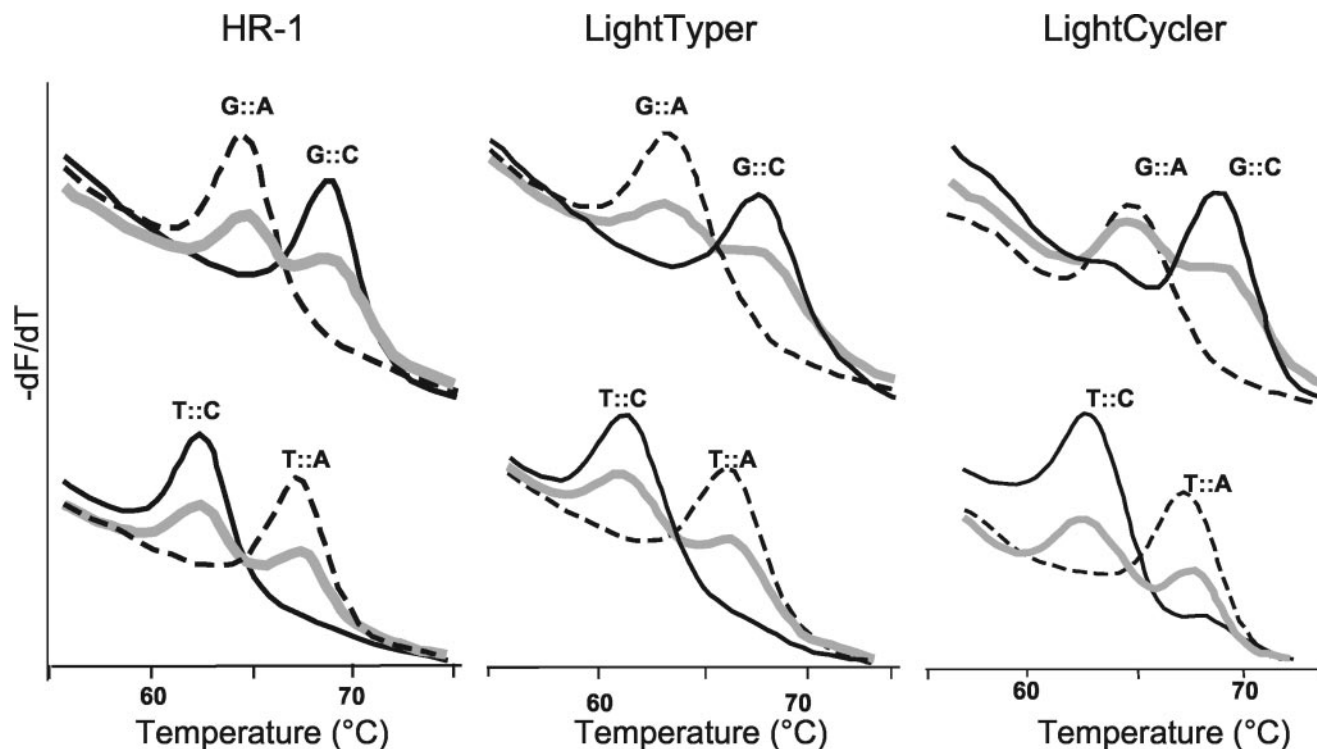


Fig. 4. Genotyping of an SNP (cystic fibrosis G542X with base designation G1756T) by use of unlabeled oligonucleotide probes on three different melting instruments.

Two different probes were compared, one complementary to the wild type (top row) and one complementary to 542X (bottom row). Melting analysis was performed on the HR-1 (left), the LightTyper (middle), or the LightCycler (right). The base pairing at the variable site is indicated. Genotypes are homozygous wild type (thin black line), heterozygous (thick gray line), and homozygous mutant (dashed line).

61.5 °C, T::A = 64.6 °C, and T::C = 60.1 °C) were 2–3 °C lower than the observed  $T_m$ s.

Genotyping of mutations around the F508 region of cystic fibrosis is shown in Fig. 5. In the top row of Fig. 5, two different SNP heterozygotes (A1648G and T1655G) are compared with the wild type. Although it was easy to distinguish the heterozygotes from the wild type, it was not easy to differentiate the two heterozygotes. The predicted  $T_m$ s (wild type = 63.2 °C, A1648G = 60.7 °C, and T1655G = 59.6 °C) were 3–4 °C below the observed transitions. Similarly, heterozygous 3-bp deletions (I507del and F508del) were easy to distinguish from homozygous samples but harder to differentiate from each other when a single wild-type probe was used (bottom row).

### Discussion

Melting analysis of unlabeled probes in PCR solutions can be used for homogeneous, closed-tube genotyping. The saturating dye, LCGreen I, is added before asymmetric PCR and monitors the melting transitions of both the PCR product and the probe–target duplexes. The usefulness of LCGreen I for multiplex melting analysis has been described previously and appears to be unique among commonly used real-time DNA dyes, such as SYBR Green I (7).

High-resolution melting analysis of double-stranded PCR products can be used to detect and differentiate

heterozygotes (7, 8). Most, but not all, SNPs can be fully genotyped by melting analysis of small amplicons (10). This method, requiring only two primers and a generic DNA dye, is the simplest method of SNP genotyping available. However, in ~4% of human SNPs, the two different homozygotes cannot be differentiated without addition of a known genotype. In addition, the method is more reliable with high-resolution melting instruments that have only become available recently.

In this report, we present a robust method for genotyping all SNPs and small deletions that does not require high-resolution melting. The ability of unlabeled probes to genotype all possible SNP base combinations was demonstrated by use of engineered plasmids to simulate homozygous and heterozygous genotypes. In addition to the amplicons and sequence variants reported here, we have also genotyped an additional 16 human genomic SNPs in 14 different amplicons with a 100% success rate. For each SNP, only three oligonucleotides are required, two PCR primers and one internal probe that is not covalently labeled with a fluorescent dye or other special functional groups. Melting transitions are monitored in the presence of LCGreen I, a dye originally designed to detect heteroduplexes (7). Multiple genotypes can be identified with a single unlabeled probe, similar to genotyping methods that monitor the melting of fluorescently labeled oligonucleotides (1–3) and in contrast to allele-

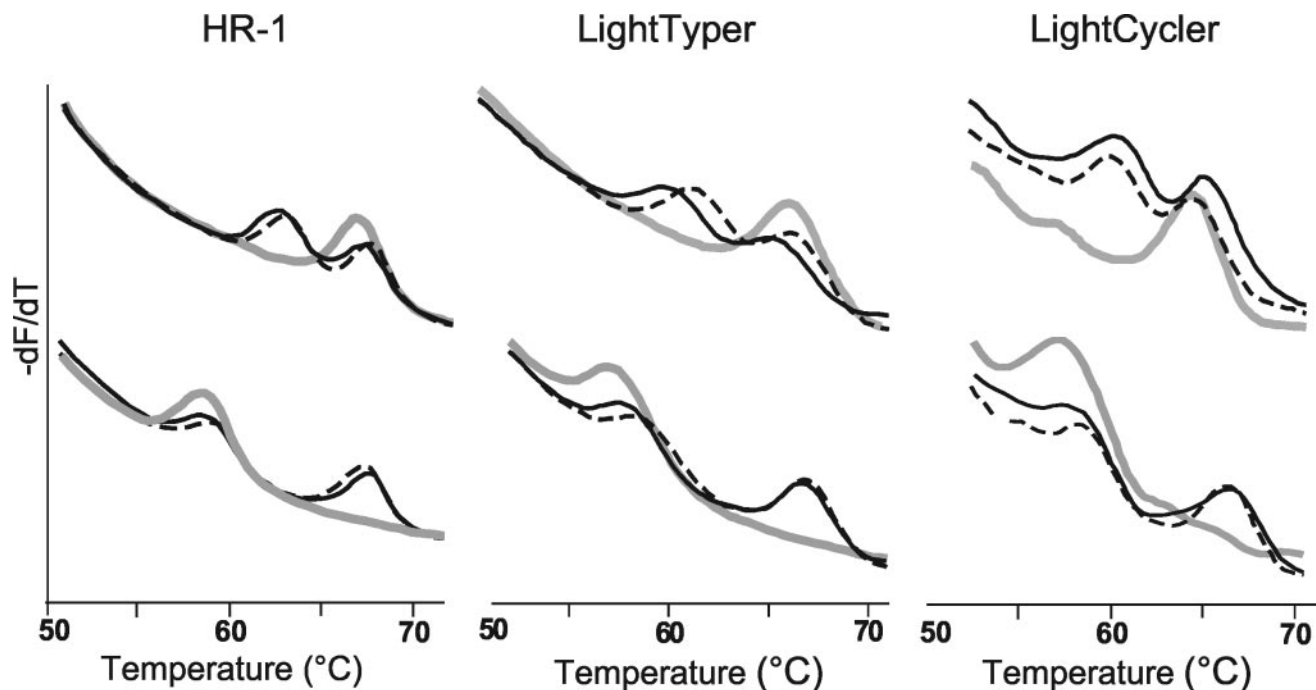


Fig. 5. Genotyping of SNPs and small deletions near the cystic fibrosis F508 region by use of unlabeled oligonucleotide probes and three different melting instruments.

In the *top row*, heterozygous A1648G (I506V; *solid black line*) and T1655G (F508C; *dashed line*) are compared with the wild type (*solid gray line*). The A1648G gives an A::C mismatch and the T1655G a T::C mismatch against the probe. In the *bottom row*, heterozygous F508del (CTT; *solid black line*) and I507del (CAT; *dashed line*) are compared with homozygous F508del (*solid gray line*). The probe was matched against the wild type. Melting analysis was performed on the HR-1 (*left*), the LightTyper (*middle*), or the LightCycler (*right*).

specific methods, in which one probe is required for each allele (4).

The robustness of asymmetric PCR has recently been questioned (25). The decreased concentration of the limiting primer lowers its  $T_m$  compared with the excess primer, a fact that may be overlooked. Indeed, with concentration taken into account, the predicted  $T_m$ s of the limiting primers used in this study were 2.3–4.9 °C below the  $T_m$ s of the excess primers. However, when the 5' ends of the limiting primers were extended so that their  $T_m$ s were 0.7–1.9 °C above the excess primers and the results from parallel experiments were compared, the probe signal (peak height on derivative plots) did not increase (data not shown). Furthermore, we experienced no difficulties in optimizing asymmetric PCR, perhaps because the asymmetry ratio used was modest (1:10).

Although there are many elegant methods for closed-tube genotyping, the oligonucleotides used are often complex, with multiple fluorescent dyes and/or functional groups (26, 27). For example, in one popular approach, a fluorescent dye, a minor groove binder, and a quencher are all covalently attached to an allele-specific probe (27). In addition, two probes are required to genotype one SNP. In contrast, SNP genotyping with an unlabeled oligonucleotide requires only one probe with no covalent modifications.

If the unlabeled probe is included in the PCR, the 3' end is blocked to prevent polymerase extension during

amplification. We used 3' phosphorylation, although a 2',3'-dideoxynucleotide, a 3'-deoxynucleotide, a 3'-3' linkage, or other nonextendable terminations, such as a 3'-spacer C3 (Glen Research) could be used. Mismatching the last two 3' bases of the probe can also be used to prevent extension.

The length and  $T_m$  of the unlabeled probe can be varied over a wide range. In the present study, melting transitions of oligonucleotides from 10 to 40 bases ranged from 48 to 91 °C. However, the most useful duplex transitions are between 55 and 70 °C. Duplexes with  $T_m$ s below this range need to be distinguished from increasing background fluorescence. Probe melting above this range may be confused, with primer-dimers often observed around 75–80 °C. The probes used for genotyping in this report were usually 27–30 bases in length. Longer probes interrogate a greater sequence region and have sharper melting transitions than shorter probes. If short probes are desired, locked nucleic acids (28) or minor groove binders (27) could likely be used. Another interesting possibility is to use multiple unlabeled probes in the same PCR, using  $T_m$  multiplexing as an alternative to color multiplexing (5).

Predicted probe  $T_m$ s were lower than actual  $T_m$ s, consistent with dye stabilization of the duplex. In general, relative stabilities were predicted by nearest-neighbor analysis. Apparent exceptions included the A::A and A::C mismatches in Fig. 3 and the A::C and T::C mismatches in

Fig. 5. Nearest-neighbor parameters may be altered in the presence of DNA-binding dyes and should be applied cautiously. The ability of melting analysis to distinguish multiple sequence alterations is well known, for example, cystic fibrosis F508C and F508del (29). However, all variants may not always be differentiated with a single wild-type probe (30).

SNP genotyping with unlabeled probes and LCGreen I does not require allele-specific PCR or real-time PCR. Only two primers, an unlabeled oligonucleotide probe, and a melting instrument are needed. Reagent costs for genotyping are low because only standard oligonucleotides and a generic dye are needed. Real-time instruments can be used for amplification and melting analysis, although there is no need for monitoring during amplification. For example, amplification and genotyping could be performed on the LightCycler (Figs. 4 and 5), although the spectrum of LCGreen I is shifted 20–30 nm to the blue away from standard fluorescein/SYBR Green I optics. Alternatively, any temperature-cycling instrument can be used for PCR with subsequent analysis on a separate instrument dedicated to melting. For example, the LightTyper can be used for high-throughput melting applications using standard 96- or 384-well plates. To better match the spectrum of LCGreen I, we modified the excitation and optics of the LightTyper. High-resolution melting on the HR-1 instrument produced the best melting curve resolution. However, unlike amplicon melting, in which resolution is paramount (7, 8), genotyping with unlabeled probes can be performed without high-resolution melting.

Homogeneous, closed-tube methods for genotyping without separation steps are attractive for their simplicity and containment of amplified products. Genotyping with unlabeled probes is robust and eliminates the need for covalently labeled fluorescent oligonucleotide probes. Combined with rapid cycle amplification (31–34), unlabeled probes provide a rapid, low-complexity method for genotyping.

We thank Noriko Kusakawa for help with the figures and for reviewing the manuscript. This work was supported by grants from the University of Utah Research Foundation, the State of Utah Center of Excellence program, and Idaho Technology.

## References

1. Lay MJ, Wittwer CT. Real-time fluorescence genotyping of factor V Leiden during rapid-cycle PCR. *Clin Chem* 1997;43:2262–7.
2. Bernard PS, Ajioka RS, Kushner JP, Wittwer CT. Homogeneous multiplex genotyping of hemochromatosis mutations with fluorescent hybridization probes. *Am J Pathol* 1998;153:1055–61.
3. Crockett AO, Wittwer CT. Fluorescein-labeled oligonucleotides for real-time PCR: using the inherent quenching of deoxyguanosine nucleotides. *Anal Biochem* 2001;290:89–97.
4. Lee LG, Connell CR, Bloch W. Allelic discrimination by nick-translation PCR with fluorogenic probes. *Nucleic Acids Res* 1993;21:3761–6.
5. Wittwer CT, Herrmann MG, Gundry CN, Elenitoba-Johnson KS. Real-time multiplex PCR assays. *Methods* 2001;25:430–42.
6. Wittwer C, Kusakawa N. Real-time PCR. In: Persing D, Tenover F, Relman D, White T, Tang Y, Versalovic J, Unger B, eds. *Diagnostic molecular microbiology; principles and applications*. Washington: ASM Press, 2003:71–84.
7. Wittwer CT, Reed GH, Gundry CN, Vandersteen JG, Pryor RJ. High-resolution genotyping by amplicon melting analysis using LCGreen. *Clin Chem* 2003;49:853–60.
8. Gundry CN, Vandersteen JG, Reed GH, Pryor RJ, Chen J, Wittwer CT. Amplicon melting analysis with labeled primers: a closed-tube method for differentiating homozygotes and heterozygotes. *Clin Chem* 2003;49:396–406.
9. Giglio S, Monis PT, Saint CP. Demonstration of preferential binding of SYBR Green I to specific DNA fragments in real-time multiplex PCR. *Nucleic Acids Res* 2003;31:e136.
10. Liew M, Pryor R, Palais R, Meadows C, Erali M, Lyon E, et al. Genotyping of single-nucleotide polymorphisms by high-resolution melting of small amplicons. *Clin Chem* 2004;50:1156–65.
11. Germer S, Holland MJ, Higuchi R. High-throughput SNP allele-frequency determination in pooled DNA samples by kinetic PCR. *Genome Res* 2000;10:258–66.
12. Germer S, Higuchi R. Single-tube genotyping without oligonucleotide probes. *Genome Res* 1999;9:72–8.
13. Highsmith WE Jr, Jin Q, Nataraj AJ, O'Connor JM, Burland VD, Baubonis WR, et al. Use of a DNA toolbox for the characterization of mutation scanning methods. I: construction of the toolbox and evaluation of heteroduplex analysis. *Electrophoresis* 1999;20:1186–94.
14. Wittwer CT, Marshall BC, Reed GH, Cherry JL. Rapid cycle allele-specific amplification: studies with the cystic fibrosis delta F508 locus. *Clin Chem* 1993;39:804–9.
15. Allawi HT, SantaLucia J Jr. Nearest neighbor thermodynamic parameters for internal G. A mismatches in DNA. *Biochemistry* 1998;37:2170–9.
16. Allawi HT, SantaLucia J Jr. Thermodynamics of internal C.T mismatches in DNA. *Nucleic Acids Res* 1998;26:2694–701.
17. Allawi HT, SantaLucia J Jr. Nearest-neighbor thermodynamics of internal A.C mismatches in DNA: sequence dependence and pH effects. *Biochemistry* 1998;37:9435–44.
18. Allawi HT, SantaLucia J Jr. Thermodynamics and NMR of internal G.T mismatches in DNA. *Biochemistry* 1997;36:10581–94.
19. Bommarito S, Peyret N, SantaLucia J Jr. Thermodynamic parameters for DNA sequences with dangling ends. *Nucleic Acids Res* 2000;28:1929–34.
20. Peyret N, Seneviratne PA, Allawi HT, SantaLucia J Jr. Nearest-neighbor thermodynamics and NMR of DNA sequences with internal A.A, C.C, G.G, and T.T mismatches. *Biochemistry* 1999;38:3468–77.
21. SantaLucia J Jr, Allawi HT, Seneviratne PA. Improved nearest-neighbor parameters for predicting DNA duplex stability. *Biochemistry* 1996;35:3555–62.
22. SantaLucia J Jr. A unified view of polymer, dumbbell, and oligonucleotide DNA nearest-neighbor thermodynamics. *Proc Natl Acad Sci U S A* 1998;95:1460–5.
23. von Ahsen N, Wittwer CT, Schutz E. Oligonucleotide melting temperatures under PCR conditions: nearest-neighbor corrections for Mg<sup>2+</sup>, deoxynucleotide triphosphate, and dimethyl sulfoxide concentrations with comparison to alternative empirical formulas. *Clin Chem* 2001;47:1956–61.
24. Ririe KM, Rasmussen RP, Wittwer CT. Product differentiation by analysis of DNA melting curves during the polymerase chain reaction. *Anal Biochem* 1997;245:154–60.

25. Sanchez JA, Pierce KE, Rice JE, Wangh LJ. Linear-after-the-exponential (LATE)-PCR: an advanced method of asymmetric PCR and its uses in quantitative real-time analysis. *Proc Nat Acad Sci U S A* 2004;101:1933–8.
26. Solinas A, Brown LJ, McKeen C, Mellor JM, Nicol J, Thelwell N, et al. Duplex Scorpion primers in SNP analysis and FRET applications. *Nucleic Acids Res* 2001;29:E96.
27. Kutyavin IV, Afonina IA, Mills A, Gorn VV, Lukhtanov EA, Belousov ES, et al. 3'-Minor groove binder-DNA probes increase sequence specificity at PCR extension temperatures. *Nucleic Acids Res* 2000;28:655–61.
28. Ugozzoli LA, Latorra D, Pucket R, Arar K, Hamby K. Real-time genotyping with oligonucleotide probes containing locked nucleic acids. *Anal Biochem* 2004;324:143–52.
29. Gundry CN, Bernard PS, Herrmann MG, Reed GH, Wittwer CT. Rapid F508del and F508C assay using fluorescent hybridization probes. *Genet Test* 1999;3:365–70.
30. von Ahsen N, Oellerich M, Armstrong VW, Schutz E. Application of a thermodynamic nearest-neighbor model to estimate nucleic acid stability and optimize probe design: prediction of melting points of multiple mutations of apolipoprotein B-3500 and factor V with a hybridization probe genotyping assay on the LightCycler. *Clin Chem* 1999;45:2094–101.
31. Meuer S, Wittwer C, Nakaguwara K, eds. *Rapid cycle real-time PCR: methods and applications*. Berlin: Springer-Verlag, 2001: 408pp.
32. Reischl U, Wittwer C, Cockerill F, eds. *Rapid cycle real-time PCR: methods and applications—microbiology and food analysis*. Berlin: Springer-Verlag, 2002:258pp.
33. Dietmaier W, Wittwer C, Sivasubramanian N, eds. *Rapid cycle real-time PCR: methods and applications—genetics and oncology*. Berlin: Springer-Verlag, 2002:180pp.
34. Wittwer C, Hahn M, Kaul K, eds. *Rapid cycle real-time PCR: methods and applications—quantification*. Berlin: Springer-Verlag, 2004:223pp.